1-1-2004

# Docosahexaenoic Acid Modulates Class I Major Histocompatibility Complex Protein Function

Kaleb Marie Hypes

# DOCOSAHEXAENOIC ACID MODULATES CLASS I MAJOR HISTOCOMPATIBILITY COMPLEX PROTEIN FUNCTION

**Thesis submitted to**
**The Graduate College of**
**Marshall University**

**In partial fulfillment of the**
**Requirements for the degree of**
**Master of Science**
**Department of Biological Sciences**

**by**

**Kaleb Marie Hypes**

**Dr. Laura Jenski, Committee Chairperson**
**Dr. Nicola LoCascio**
**Dr. Susan Jackman**

**Marshall University**

**11 June 2004**

# ABSTRACT

## DOCOSAHEXAENOIC ACID MODULATES CLASS I MAJOR HISTOCOMPATIBILITY PROTEIN FUNCTION

**By Kaleb Marie Hypes**

Fatty acids influence immune responses, but how this occurs at the molecular level is not understood. Class I major histocompatibility complex molecules (MHC I), transmembrane proteins required for antigen presentation to T cell receptors, each consist of a 45kDa α chain noncovalently associated with a 12-kDa $\beta_2$-microglobulin ($\beta_2$m) molecule. Docosahexaenoic acid's (DHA) effect on the binding of $\beta_2$m and anti-MHC I monoclonal antibodies (Mab) was measured. EL4 and RMA-S cells were cultured 48 hours with 0-45μM DHA or oleic acid. Murine to human $\beta_2$m exchange and Mab binding were assessed by fluorescence flow cytometry. DHA-treated cells showed increased fluorescence (greater $\beta_2$m binding and Mab binding) compared to untreated and oleic acid-treated cells. The addition of α-tocopherol to these fatty acid treatments eliminated the DHA-associated increase in fluorescence. DHA's effect on the cell membrane may alter the conformation of MHC I affecting antigen presentation to $CD8^+$ T-lymphocytes and altering immune response.

## ACKNOWLEDGMENTS

The author wishes to acknowledge the following individuals for their contributions:

My mother, Kaluwa Schoen, for constant love and support. I couldn't have made it this far without you.

My soon-to-be husband, Brad Pauley, for always being there when I need you, for always listening, and for your late-night lab trip escorts.

Dr. Laura Jenski, my mentor and advisor, for guidance, patience, and support. My experience in the lab has been exceedingly valuable.

Jennifer Bush, my friend and colleague, for keeping me sane in the lab and for constant support and assistance.

All the friends and lab members that have made my time at Marshall enjoyable and entertaining: Kristin, Tiffany, Chris, Rebecca, Kamilla, and Hilal.

The faculty and staff of the department of biological sciences, Marshall University, for education, enlightenment, and encouragement.

Thank you all.

## TABLE OF CONTENTS

## LIST OF FIGURES

# INTRODUCTION

The objective of this study was to examine the effects of docosahexaenoic acid (DHA) on the structure and function of class I major histocompatibility complex (MHC I) proteins. This was accomplished by examining murine to human $\beta_2$-microglobulin exchange, anti-MHC I monoclonal antibody binding, and peptide-induced MHC I expression in DHA-treated cells as compared to untreated and oleic acid treated cells.

## Major Histocompatibility Complex (MHC):

The immune system relies on many regulatory mechanisms that govern its ability to respond to infectious agents, and one such mechanism is the MHC. The MHC has long been known to be involved in the rejection of organ and bone marrow transplants. In the mid-1930s, Gorer and Snell determined that a molecule in foreign tissue caused the rejection of transplants (1). It was first believed that this molecule was a soluble antigen that stimulated an immune response. It was not until much later, in the 1970's, that Zinkernagel observed that the soluble antigen alone was not enough to stimulate an immune response, but that antigen had to be accessible through another molecule, MHC proteins (2). Eventually, it was learned that MHC proteins have many important functions including the control and development of CD8+ T cells, the induction of self tolerance in the thymus, immune surveillance against pathogens and tumors, and the acceptance or rejection of transplants (3).

The genes responsible for coding the MHC proteins (MHC genes) are located on a long continuous stretch of DNA on chromosome 6 in humans and chromosome 17 in

mice (1). These genes encode three major classes of MHC molecules. Class I MHC molecules are glycoproteins found on all nucleated cells that present peptide antigens to CD8+ T cells. CD8+ T lymphocytes, or cytotoxic T lymphocyte (CTL), are generally distinguishable by the CD8 membrane glycoproteins on their cell surface. CTLs target and destroy cells whose MHC I molecules display "foreign," or non-self, antigens. The CTL has a vital function in eliminating virus-infected cells, tumor cells, and cells of a foreign tissue graft. Class II MHC molecules are expressed primarily on such antigen-presenting cells as macrophages, dendritic cells, and B cells. MHC II molecules present exogenous peptides to CD4+ T cells. These T cells, referred to as T helper cells, are generally distinguishable by the CD4 membrane glycoproteins on their cell surface. T helper cells recognize antigen-MHC II complexes and secrete cytokines. These cytokines help to activate B cells, CTLs, and macrophages that then participate in the immune response. Class III MHC genes encode secreted proteins that have immune functions, including components of the complement pathway and molecules involved in inflammation (1).

Human class I MHC molecules have been named human leukocyte antigen (HLA), and there are three different forms of HLA molecules, HLA-A, HLA-B and HLA-C. There are also three different forms of murine H-2 class I MHC molecules, H-2D, H-2K, and H-2L. The H-2 molecules can be further distinguished by haplotype, that is, the set of alleles of linked genes present on one parental chromosome (1). An individual receives one maternal haplotype and one paternal haplotype. These haplotypes are co-dominantly expressed, which yields a very high degree of polymorphism among the H-2 molecules (1). Inbred mice are homozygous at the H-2 locus because the

maternal and paternal haplotypes are identical; therefore all offspring express identical haplotypes. The MHC haplotype expressed by these strains of inbred mice is designated by an arbitrary superscript (H-$2^b$, H-$2^d$) (1).

The MHC class I molecule is comprised of a polymorphic 45-kDa heavy chain, a non-covalently associated 12-kDa protein called $\beta_2$-microglobulin ($\beta_2$m) and a short peptide of 8-10 amino acids in length. Class I chains require full assembly with $\beta_2$m and peptide to be stably expressed on the cell membrane (4). The heavy chain is made up of three distinct domains, $\alpha$1, $\alpha$2, and $\alpha$3, each containing approximately 90 amino acids (1). The $\alpha$1 and $\alpha$2 domains form the peptide-binding groove where the peptide antigen is bound (Fig. 1). MHC I molecules also have an alpha helical transmembrane region of about 25 hydrophobic amino acids followed by a short stretch of hydrophilic amino acids, and finally a short cytoplasmic tail made up of 30 amino acids (1).

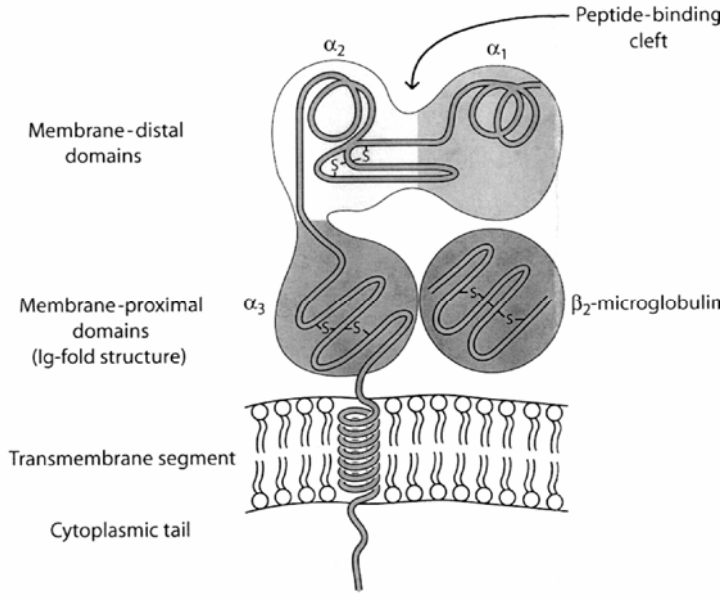


**Figure 1.** The class I MHC molecule. MHC I consists of a 45-kDa heavy chain and a 12-kDa light chain (β2m), a hydrophobic transmembrane region, a cytoplasmic tail. The heavy chain is comprised of three

extracellular domains: α1, α2, and α3. Disulfide bonds are present where indicated. Figure taken from Reference 1.

Throughout the presentation of antigenic peptide by MHC I to T cell receptors (TCR) (Fig. 2), the peptide and several amino acid residues of the MHC I α-chain contact the TCR (5). Consequently, the conformation of the α-chain is critical in interacting with the TCR. The three-dimensional structure of membrane-bound H2-$K^b$ shows that the extracellular portion of MHC I is positioned on the membrane such that β2m is in contact with the lipid layer while the peptide binding groove faces away from the membrane toward the TCR (6). Given that MHC I is a transmembrane protein and its extracellular domains come in contact with the plasma membrane, it is important to understand how lipids in the plasma membrane may affect the structure and thus the function of MHC I.

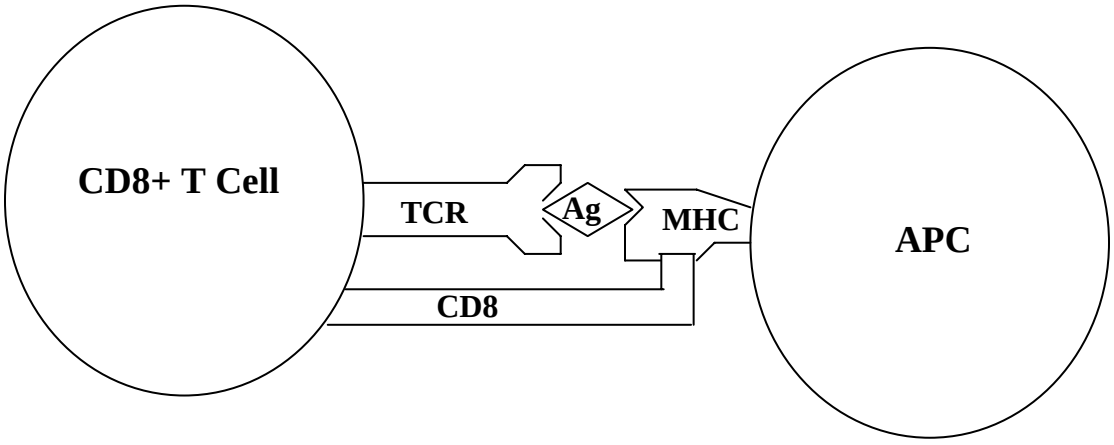


**Figure 2.** Schematic of an antigen presenting cell (APC) interacting with a CD8+ T cell. The T cell receptor (TCR) of the CD8+ T cell is binding to the α1/α2/peptide complex while the CD8 receptor of the CD8+ T cell binds to the α3 domain of MHC I. Figure adapted from Reference 1.

**$\beta_2$-microglobulin:**

$\beta_2$-microglobulin is the 12-kDa protein that is non-covalently associated with MHC class I heavy chain. Until recently, it was thought that $\beta_2$m was required for the proper folding and expression of MHC I on the cell surface. The general consensus was that in the absence of $\beta_2$m, MHC molecules underwent architectural editing in the endoplasmic reticulum (ER) and were lost to cytosolic degradation. However, functional class I molecules do assemble with peptides in the absence of $\beta_2$m and form CD8+ T cell epitopes (7). These $\beta_2$m-free MHC I molecules permit the development of CD8+ T cells that are able to elicit a lytic response and mediate tumor-specific immunity as well as transplant rejection (7).

Murine $\beta_2$m can readily exchange with human $\beta_2$m and bovine $\beta_2$m. In fact, both human and bovine $\beta_2$m have a higher affinity for murine class I MHC molecules than does murine $\beta_2$m (8). Many *in vitro* studies using murine systems culture cells in the presence of fetal bovine serum (FBS), which is a rich source of bovine $\beta_2$m. Thus, problems in interpretation could occur if it assumed that the murine cells studied possess fully murine MHC I molecules. It is for this reason that all cells used in this study were cultured in serum-free medium in the absence of any exogenous $\beta_2$m.

It has been observed that the rate of $\beta_2$m exchange on cell surface class I MHC molecules varies widely depending on the peptide ligand's structure and affinity (9). This finding indicates that there is significant "cross-talk" between the peptide binding and $\beta_2$m binding regions of the MHC I heavy chain (9). It also tells us that there is a range of MHC I "structure" that is acceptable to the cells and apparently functional.

**Peptide:**

The α1 and α2 domains of the class I heavy chain form a peptide binding groove made up of a platform of antiparallel β-pleated sheets and two alpha helices (1). The dimensions of the peptide-binding groove is about 1 x 2.5 nm and it can accommodate a peptide of 8-10 amino acids in length (10). These peptides are tightly bound in the groove. Both N and C termini of the peptide interact with MHC residues deep within the groove (10). Certain side chains of peptide amino acids interact with corresponding MHC residues forming pockets that vary in location and shape depending on the allelic form of the molecule. Thus, the polymorphism of class I MHC molecules is reflected in the peptide binding groove's specificity. It has been shown that each MHC class I allelic product has its own peptide preference (10). For instance, H2-$K^b$ molecules accommodate peptides of 8 amino acids in length whose anchor residues are often phenylalanine (position 5) and leucine (position 8) (10). The natural ligands of the molecule were found to include RGYVYQGL (11), SIINFEKL (12), and HIYEFPQL (13).

In general, class I MHC peptides are derived from processed endogenous proteins that bind to newly synthesized heavy chain within the ER. Intracellular proteins are targeted for degradation by ubiquitination and degraded into peptide pieces by proteasomes. Peptides are then transported from the cytosol into the lumen of the rough ER by TAP (transporter associated with antigen processing) by a process that requires the hydrolysis of ATP. From there, the peptides assemble with class I MHC molecules aided by chaperone molecules. Calnexin, a resident membrane protein in the ER, binds to a free class I α chain and promotes its folding. When $\beta_2$m binds to the α chain, calnexin is released, and the class I complex associates with calreticulin and with the TAP-associated

protein tapasin. Tapasin draws the TAP transporter into proximity with the class I molecule and allows it to acquire an antigenic peptide (Fig. 3).

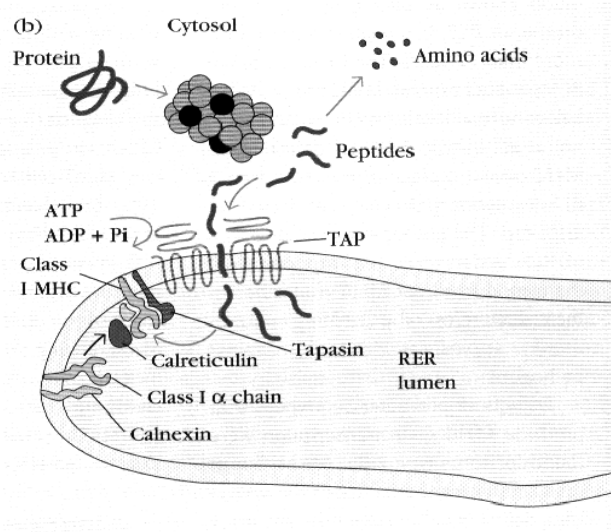


**Figure 3.** Endogenous peptide processing through cytosolic pathway. The proteasome degrades an intracellular protein into peptide pieces. Peptides are then transported by TAP into the rough ER lumen where tapasin brings TAP in close proximity with the MHC I complex so that peptide may bind in the peptide groove. Figure taken from Reference 1.

However, exogenous peptides can also bind to class I heavy chains (14). This finding is critical in the function of peptide-based vaccines (15) and may also be important in the "peptide regurgitation" pathway of antigen presentation (16) in which processed antigen is released from the cells and binds to MHC I on the cell surface.

The exact mechanism by which exogenous peptide binds to class I MHC molecules is not yet fully understood, but several pathways have been proposed. First, the cell must degrade these exogenous peptides, and this is proposed to occur through any of three pathways. First, the peptides could be released from endosomes into the cytosol and degraded by proteasomes leading to their transport by TAP into the ER. Second, the peptides could be degraded and loaded in endosomes containing recycled surface MHC I.

Third, the peptide could be degraded inside the endosome and then regurgitated back outside of the cell where they bind class I molecules (17).

Once processed, the exogenous peptides must be presented by class I molecules. One proposed mechanism by which this might occur is that the peptides bind to class I complexes in a pre-Golgi compartment, promoting their release to the cell surface (17). Another possibility is that exogenous peptides bind empty class I molecules on the cell surface or exchange with low-affinity peptides (18). Also, it has recently been shown that incubation with exogenous peptides in TAP-deficient cells can induce the release of nascent class I molecules from the ER, suggesting that the peptide acts inside the ER to induce MHC I maturation from the ER to the cell surface (17). It is known that exogenous peptides can enter into intracellular compartments in a TAP-independent way (19). Within these ER compartments, the peptides can bind to de novo-synthesized class I molecules (18). Again, the exact role of exogenous peptide presentation by MHC I in the immune response is not yet understood.

**Docosahexaenoic acid:**

Docosahexaenoic acid (DHA) is an ω-3 polyunsaturated fatty acid (PUFA) with 22-carbons and 6 double bonds (Fig. 4). DHA is the longest and most unsaturated PUFA found commonly in biological systems, and is found in abundance in marine fish oils. The positive effects of the dietary intake of DHA were first observed during an epidemiological study of Arctic Inuit Eskimos that showed a low incidence of coronary heart disease. Since the Eskimo diet consisted primarily of marine mammals and fish, it was deduced that some component in the marine diet, which is not prevalent in a Western

diet, was exhibiting protective effects against certain diseases such as heart disease (20,21). Since then, DHA's presence has been positively linked to the prevention or treatment of numerous human diseases such as heart disease (22), cancer (23), rheumatoid arthritis (24), asthma (25), lupus (26), alcoholism (27) and many others.

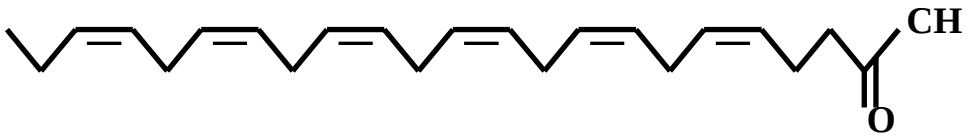


**Figure 4.** Molecular Structure of DHA.

Omega-3 fatty acids are named such due to the position of the last double bond being three carbons from the methyl (or omega) end of the acyl chain. In nature, DHA is produced by unicellular algae through a complex series of elongation and desaturation reactions. Marine crustaceans called copepods then consume these algae, and fish consume the copepods leading to high amounts of DHA in fish oils (28).

In mammals, DHA is only found in abundance in certain tissues, such as synaptosomes (29), sperm (30), and the retinal rod outer segment (31). In these membranes, DHA can approach 50 mol% of the total phospholipid acyl chains (32). Limited tissue distribution of high DHA levels implies a specialized but undefined role for DHA in these cells (33). The high levels of DHA in these tissues are not changed by increased dietary intake of DHA (32). However, in other tissues where DHA is often found below 5 mol% of the total phospholipid acyl chains, DHA can be enriched two to ten fold through dietary supplementation (32). It is in these diet-sensitive cells that DHA probably exhibits its numerous health benefits (33).

DHA readily incorporates into a variety of cells, predominantly into the phospholipids of the plasma membrane (23) and mitochondria (34, 35). It is estimated that DHA prefers phosphatidylethanolamine over phosphatidylcholine by about 5.7 times in T27A leukemic cells (33). Once incorporated into the cell membrane, DHA has dramatic effects on membrane stability, fluidity, and permeability.

DHA's multiple rigid double bonds causes distortion in the packing of phospholipid acyl chains. Consequently, there is a reduction in intra- and inter-molecular van der Waal's interactions, which subsequently decreases membrane stability (33). An increase in plasma membrane fluidity in animal models and cultured cells has also been associated with DHA enrichment (36, 37, 38, 39). DHA increases membrane permeability two to three fold more than oleic acid (40). This increase in permeability is probably due to the wedge shape of DHA-containing phospholipids (small head group and wide acyl tail) (41). The looser packing of lipids in the membrane would allow deeper penetration of water and solutes into the lipid bilayer (41). The looser packing may also favor the insertion, movement, clustering, or conformational change of proteins into DHA-rich portions of the membrane (42).

The effect of DHA incorporation into various phospholipids on membrane protein function is not yet fully understood. DHA's effect on membrane properties may cause changes in the properties of membrane proteins. Such changes could affect the function of the protein. The effects of DHA on several membrane proteins, including rhodopsin, have been thoroughly studied.

Rhodopsin is a membrane protein of the rod photoreceptor cell in the retina of the eye. It catalyses the only light sensitive step in vision. When light is absorbed, a change

in the conformation of rhodopsin triggers a sequence of reactions that leads to a nerve impulse. This is transmitted to the brain via the optical nerve. The presence of DHA in these cell membranes was found to enhance the light-triggered conformational change in rhodopsin thereby enhancing the initial neuronal response of the eye to light (43).

This study will focus on the effect that the incorporation of DHA into phospholipids has on the structure and function of the transmembrane protein MHC I.

**Objective:**

The objective of this study is to examine the effects of cellular DHA incorporation on MHC I expression, conformation and function as shown by monoclonal antibody, $\beta_2$m, and peptide binding. My hypothesis is that the various membrane effects of DHA will cause the transmembrane protein MHC I to have an altered conformation thereby affecting the function of the molecule. It is also possible that the emergence of MHC I onto the cell surface will be altered by DHA enrichment (44,45). The overall goal of this work is to shed light on how the effects of DHA on MHC I may alter immune response in such a way as to prevent cancer and autoimmune disease.

## MATERIALS

The following materials and equipment were used during this research and are organized below by descriptive categories.

**Antibodies and Labels:**

- Biotin-conjugated mouse anti-mouse H-2K$^b$ monoclonal antibody, clone AF6-88.5 (#553568), BD Pharmingen, Palo Alto, California.
- Fluorescein isothiocyanate (FITC)-conjugated mouse anti-mouse H-2K$^b$ monoclonal antibody, clone AF6-88.5 (#553569), BD Pharmingen.
- Biotin-conjugated mouse anti-mouse H-2D$^b$ monoclonal antibody, clone 28-14-8 (#553601), BD Pharmingen.
- Biotin-conjugated mouse $IgG_{2b}$, κ monoclonal immunoglobulin isotype control (#559531), BD Pharmingen.
- FITC-conjugated mouse $IgG_{2b}$, κ monoclonal immunoglobulin isotype control (#559532), BD Pharmingen.
- Streptavidin-allophycocyanin conjugate (#554067), BD Pharmingen.
- Goat anti-mouse IgG (whole molecule), FITC conjugate, affinity-isolated antibody (#F2012), Sigma-Aldrich, St. Louis, Missouri.
- Monoclonal anti-human Beta-2-microglobulin, clone BM-63 (#M7398), Sigma-Aldrich.
- Beta-2-microglobulin from human urine (#M-4890), Sigma.

**Cell Culture:**

- EL4 cell line, American Type Culture Collection, Manassas, Virginia (#TIB-39, strain C57BL/6N).
- RMA-S cells graciously provided by Dr. Peter Cresswell (Professor of Immunobiology and Cell Biology, Yale University) and Dr. Ted Hansen (Professor of Genetics, Pathology and Immunology, Washington University)
- HyQ-CCM 1 serum-free medium for hybridomas, HyClone, Logan, Utah (#SH30043), stored at 4°C.
- Medium supplemented with 100 units penicillin G and 100 µg streptomycin per ml (Gibco BRL Life Technologies, #15140).
- Phosphate buffered saline, pH 7.2, Gibco Invitrogen, #20012-027.
- Bovine serum albumin (#A-7906), Sigma.
- Trypan blue, Sigma, #T6146.
- α-Tocopherol (#T 3251), Sigma.
- Peptide SIINFEKL (serine, isoleucine, isoleucine, asparagine, phenylalanine, glutamic acid, lysine, leucine), Biomer Technology, Concord, California (#3J17-2-MSA).

**Fatty Acids:**

- DHA, Nu-Chek Prep, Elysian, Minnesota, #U-84-A.
- Oleic acid, Nu-Chek Prep, #U-46-A.

- Hexane used as solvent (29-325-3), Aldrich, Milwaukee, Wisconsin.

**Reagents:**

- Absolute Ethanol (E702-3), Aldrich.

**Equipment:**

- Pipetters. Rainin Pipetman. 1000 µl capacity, # P-1000; 200 µl capacity, # P-200, 20 µl capacity, # P-20.
- Vortex. Fisher Genie 2. Fisher Scientific, Pittsburgh, Pennsylvania, # 12-812.
- Centrifuge. IEC Centra CL3R. International Eqipment Company, Needham Heights, Massachusetts, # 3755.
- Flow Cytometer. Epics Altra. Beckman Coulter, Inc., Miami, Florida, # 6605563.
- Pipet pump. Drummond Pipet-aid. Drummopnd Scientific Company, Broomall, Pennsylvania, # 4-000-110.
- Laminar flow hood. Safeaire biological safety cabinet. Fisher Hamilton L.L.C., Two Rivers, Wisconsin, # 54L392.
- Incubator. Humidified incubator, set to 37.5°C with 5% $CO_2$. Heraeus Instruments, South Plainfield, New Jersey, # B-5060.

**Supplies:**

- Small cell culture flasks. Falcon 50-ml polystyrene tissue culture treated flasks with plug caps. Becton Dickinson Labware, Franklin Lakes, New Jersey. # 353014.
- Large cell culture flasks. 75-cm2 cell culture treated flasks with plug caps. Corning Incorporated, Corning, New York. # 430720.
- Centrifuge tubes. 15-ml and 50-ml Fisherbrand polystyrene centrifuge tubes. Fisher Scientific. #s 05-539-2 and 05-539-10.
- Capped culture tubes. Fisherbrand 75-$mm^2$ polystyrene tubes. Fisher Scientific. # 202109428.
- 5-ml glass test tubes. Fisher Scientific. # 14-961-26.
- Pipettes. Costar stripette polystyrene pipettes. Corning Incorporated. 5-ml: #4487; 10-ml: # 4488; 25-ml: #4489; 50-ml: # 4490.
- Pipette tips. Fisherbrand Redi-Tip general purpose tips. Fisher Scientific. Yellow 1-200-µl tips # 21-197-8G; blue 101-1000-µl tips # 21-197-8F.
- Tissue culture plate, 24-well, flat bottom with low evaporation lid. Becton Dickinson Labware. #353047.
- Microcentrifuge tubes. Fisherbrand 1.5-ml tubes. Fisher Scientific. # 05-408-129.

## METHODS

**Cell Culture**:

In sterile 75-$cm^2$ flasks, EL4 and RMA-S cells were cultured in serum-free medium supplemented with 100 units penicillin G and 100 µg streptomycin per ml in a humidified incubator at 5% $CO_2$. The cells were maintained at a passage rate of 2-3 days. Cells were harvested by centrifuging at 1500 rpm (450 x g) for 10 minutes. Upon harvesting, cell counts were performed using a hemocytometer and trypan blue stain. Twenty-five microliters of 0.04% trypan blue was mixed with 25 µl of cell suspension and allowed to incubate for 30 seconds. Fifty microliters of PBS was then added, and the cells were examined under a hemocytometer. Cells with a viability of 90% or better were used in assays. Once cells were harvested and counted, they were suspended in fresh serum-free medium at a concentration of approximately 1.0 x $10^6$ cells/ml.

**Fatty Acid Incubation:**

Docosahexaenoic acid and oleic acid were dissolved in hexane at a concentration of 10 mg/ml and stored in brown vials at –30°C. The vials were opened under a stream of nitrogen gas to prevent oxidation of the fatty acid. For 1 ml of 200 µM DHA, 6.56 µl of DHA (in hexane) was dried under nitrogen for about 5 minutes. The DHA was then dissolved in 10 µl of 100% ethanol and dripped slowly into 990 µl of serum-free medium while vortexing. An additional 1 ml of serum-free medium was added for a final concentration of 100 µM DHA. For 1 ml of 200 µM oleic acid, 5.75 µl of oleic acid (in hexane) was dried under nitrogen and dissolved in 10 µl of 100% ethanol. It was then

dripped slowly into 990 µl of serum-free medium. An additional 1 ml of serum-free medium was added for a final concentration of 100 µM oleic acid.

Cells were treated with different concentrations of fatty acid in a 24-well plate for 48 hours at 37°C. Approximately 5.0 x $10^5$ cells in 500 µl of serum-free medium were placed in each well with 0, 35, 40 and 45 µM fatty acid. Serum-free medium was added to bring the final volume of each well to 1.5 ml, and 0.5% EtOH was added to each well. After the two-day incubation, treated cells were harvested by centrifuging at 1500 rpm for 10 minutes and washed in PBS containing 1% BSA. EL4 cells were used in the monoclonal antibody binding assays, beta-2 microglobulin assay, MHC turnover assay, and the α-tocopherol assay. RMA-S cells were used in the peptide-induced MHC I expression assay.

**Monoclonal Antibody Binding Assays:**

Once EL4 cells were treated with fatty acid and washed, they were resuspended in 200 µl PBS with 1% BSA at a concentration of about 1.0 x 10^6 cells/ml. One microgram of biotinylated anti-H-$2K^b$ (Clone AF6-88.5) or anti-H-$2D^b$ (Clone 28-14-8) was added to the cell suspension that was then incubated on ice for 30 minutes. Some samples used as negative controls were incubated with 1 µg of biotinylated mouse $IgG_{2b}$, κ immunoglobulin isotype control. The cells were centrifuged at 1500 rpm at room temperature for 10 minutes and washed with 500 µl PBS containing 1% BSA. The cells were resuspended in 200 µl PBS with 1% BSA. Then 0.4 µg of streptavidin-allophycocyanin was added to the cells suspension and incubated on ice for 30 minutes. The cells were centrifuged at 1500 rpm at room temperature for 10 minutes and washed

with 500 µl PBS containing 1% BSA before being resuspended in 1ml PBS containing 1% BSA for analysis by flow cytometry. The samples were stored on ice and covered with aluminum foil for protection from light.

Unless it is stated otherwise, all conditions for washing and resuspending the cells are the same in each assay, as are the approximate cell concentrations in suspension and the storage of the samples during analysis.

**Beta 2-microglobulin Binding Assay:**

Once EL4 cells were treated with fatty acid and washed, they were resuspended in 200 µl PBS containing 1% BSA. The cells were then incubated on ice for 30 minutes with 5 µg of human beta-2 microglobulin and washed again. The human beta-2 microglobulin was stored at -30°C in 50 µl aliquots at 0.1 µg/µl. The cells were then resuspended in 200 µl PBS with 1% BSA and incubated with 1.0 µg monoclonal anti-human beta-2 microglobulin for 30 minutes on ice. The anti-human beta-2 microglobulin stock solution (1.6 mg/ml) was stored at -30°C. Fresh 1:10 dilutions of the reagent were prepared for each experiment. Those samples used as negative controls were not incubated with anti-human beta-2 microglobulin. Following another wash, the cells were resuspended in 250 µl PBS with 1% BSA and incubated with 1.1 µg FITC-conjugated goat anti-mouse IgG for 30 minutes on ice. This reagent was stored at 4°C. After a final wash, the cells were analyzed by flow cytometry.

**Peptide-induced MHC I expression:**

RMA-S cells were treated with DHA and oleic acid as previously described. After 36 hours of incubation with the fatty acids at 37°C, 500 μM (39.47 μl at 0.25 μg/μl) peptide (SIINFEKL) was added to the cells for the remaining 12-hour incubation. The SIINFEKL peptide (serine, isoleucine, isoleucine, asparagine, phenylalanine, glutamic acid, lysine, leucine) was dissolved in PBS and stored at -30°C in 200 μl aliquots at a concentration of 0.25 μg/μl. The cells were washed and resuspended in 200 μl PBS containing 1% BSA. The cells were incubated on ice for 30 minutes with 1 μg (2.0 μl) FITC-conjugated anti-H-2K$^{b}$ (Clone AF6-88.5) or biotinylated anti-H-2D$^{b}$ (Clone 28-14-8). After washing, the cells incubated with biotinylated 28-14-8 were incubated 30 minutes on ice with 0.3 μg (3.0 μl) streptavidin-APC, washed again, resuspended in 1 ml PBS containing 1% BSA, and then analyzed by flow cytometry. The cells incubated with FITC-AF6-88.5 were immediately washed, resuspended in 1 ml PBS containing 1% BSA and analyzed by flow cytometry. Samples of cells from each fatty acid treatment that did not undergo incubation with peptide were used as negative controls.

**α-Tocopherol Assay:**

EL4 cells were incubated in fatty acids as described previously, except that the 0.5% ethanol in each well contained 15 μg/ml α-tocopherol. The cells were incubated 48 hours at 37°C, washed, and resuspended in 200 μl PBS containing 1% BSA. One microgram (2.0 μl) of biotinylated AF6-88.5 or 28-14-8 antibody was added, as well as 1.0 μg (2.0 μl) of biotinylated isotype control antibody to the negative control samples. The samples were incubated on ice for 30 minutes, washed, and resuspended in 200 μl

PBS containing 1% BSA. Then 0.3 µg (3.0 µl) streptavidin-allophycocyanin was added to each sample and incubated on ice an additional 30 minutes. After a final wash, the cells were resuspended in 1 ml PBS containing 1% BSA and analyzed by flow cytometry.

**Flow Cytometry:**

A Beckman Coulter Altra flow cytometer with Expo32 MultiComp software was used to analyze all samples. Those samples that were analyzed with an FITC-conjugated antibody were excited at 488 nm with an Argon laser and emitted fluorescent light in the 525 nm range was collected, as well as forward and side scatter light. Those samples labeled with the biotin-streptavidin-APC complex were excited at 633 nm with a red HeNe laser and fluorescence in the 675 nm range was collected, as well as forward and side scatter light. In all cases, 10,000 events were collected and then analyzed using Expo32 Analysis Software version 1.2. Logarithmic plots of each fatty acid treatment were superimposed with the corresponding control sample (untreated cells). The control sample was then subtracted from each treatment plot, and the Overton percent was calculated by determining what percentage of the treatment plot was more positive than the control plot, where positive is defined as higher fluorescence. These Overton percents were plotted using Sigma Plot 2000 and statistical significance ($P \leq 0.05$) was determined by one-way ANOVA using Sigma Stat 3.0.

## RESULTS

DHA's effect on MHC I function was measured by examining murine to human $\beta_2$m exchange, anti-MHC I monoclonal antibody (Mab) binding, and Mab binding to peptide-induced MHC I on the cell surface. EL4 and RMAS cells were cultured for 48 hours with 0-45 μM DHA or oleic acid, and $\beta_2$m binding and Mab binding were assessed by fluorescence flow cytometry. DHA treated cells were compared to untreated cells by superimposing their histograms, which were generated by flow cytometry. Overton percents were calculated by Expo32 software to determine what percentage of the treatment plot was more positive than the control (untreated) plot, where positive is defined as higher fluorescence (more binding).

### DHA Dose Response:

The optimal range of DHA concentrations was determined by a curve measuring response to a series of doses. A range of 20-55 μM DHA was tested on EL4 cells (Fig. 5). The range of DHA concentrations used in impending experiments, 35-45 μM DHA, was selected based on the greatest effect on the binding of β2m, peptide and anti-MHC I Mab while maintaining cell viability. This range was initially determined by the $\beta_2$m binding assay, but proved to be optimal for Mab and peptide binding assays as well. The result of 35 μM DHA treatment was 22% more fluorescence (i.e. resulted in more binding) than no treatment. The 40 μM and 45 μM DHA treatments were 44% and 73% more fluorescent, respectively. All logarithmic fluorescent plots were gated on viable cells shown by scatter plots (Fig. 6).

A distinct shift in the light scatter pattern of DHA-treated cells was revealed by scatter plots, indicating increased size and complexity of the cellular membrane (Fig. 6). Cell viability decreased from 87% with no DHA to 41% with 45 μM DHA. Oleic acid had no significant effect on the scatter pattern of the cells (Fig. 6).

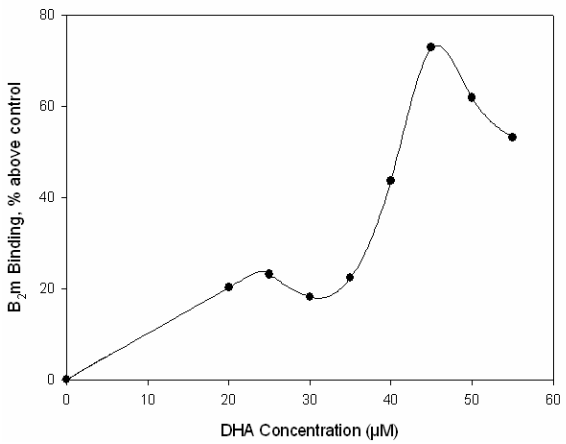


**Figure 5.** Dose response curve for EL4 cells treated with DHA. Cells were treated with 0-55 μM DHA for 48 hours at 37°C. Murine to human $\beta_2$m exchange was measured for each treatment. Logarithmic plots were gated on live cells as determined by scatter plots. Overton percent was calculated using Expo32 software by overlaying each treatment plot with the untreated plot, thus yielding the percentage of cells that are more positive than the control (untreated cells) where positive is defined as higher fluorescence. This graph is representative of a single experiment.

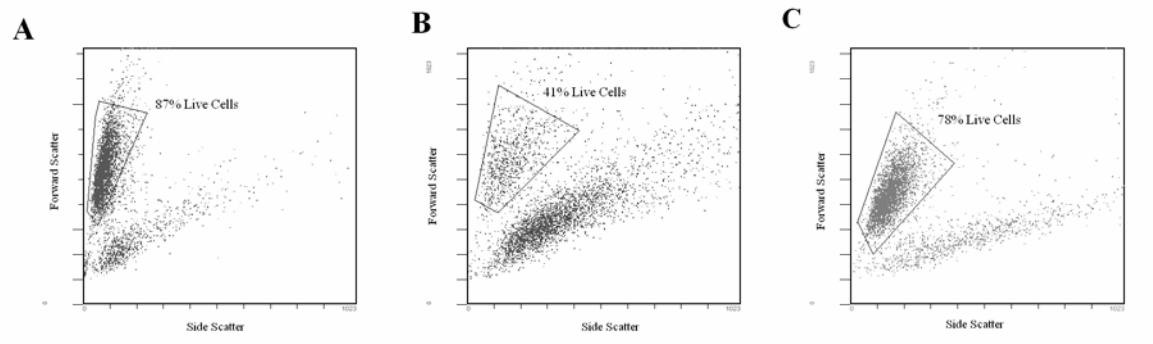


**Figure 6.** Scatter plots of untreated, DHA-treated and oleic acid-treated EL4 cells. **A)** Two-dimensional plot of forward versus side (90°) laser light scatter of untreated EL4 cells. The gate defines the cell population analyzed in Figure 5 (87%). **B)** 45 μM DHA treated EL4 cells, 41% gated. **C)** 45 μM Oleic acid treated EL4 cells, 78% gated. These graphs are representative of a single experiment**.**

**$\beta_2$m Dose Response:**

The optimal concentration of human $\beta_2$m to be exchanged with murine $\beta_2$m was determined by a dose response curve. A range of 3 to 7 µg human $\beta_2$m was added to EL4 cells (Fig. 7). The optimal amount of human $\beta_2$m was determined to be 5 µg (50 µl of 0.1 µg/µl stock solution), which was 91% more fluorescent than the negative control.

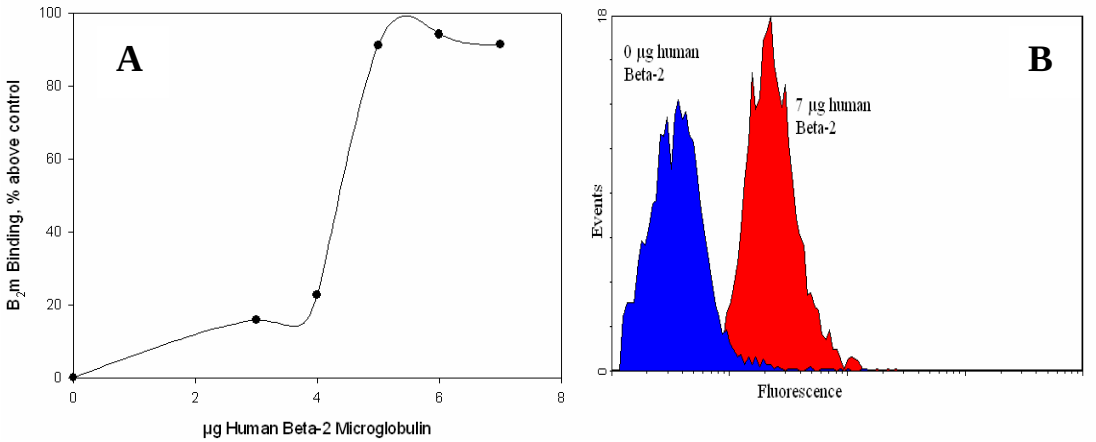


**Figure 7.** Human $\beta_2$m dose response curve. **A)** Dose response curve for human $\beta_2$m. Human $\beta_2$m (3-7 µg) was added to EL4 cells and allowed to incubate 30 minutes on ice. The cells were stained for $\beta_2$m binding as previously described, and their fluorescence was measured by flow cytometry. Overton percents were calculated by determining the percentage of cells in each treatment plot that were more fluorescent than the untreated cells. Higher percentages (higher fluorescence) indicate increased $\beta_2$m binding. **B)** Example of overlay plot. EL4 cells were treated as described above. Human β2m (7.0 µg) binding is displayed by the peak on the right. The peak on the left displays the negative control (no human β2m added).

**DHA increases $\beta_2$m binding to MHC I on the cell surface:**

The effect of DHA and oleic acid on $\beta_2$m binding was determined by fluorescent flow cytometry as previously described. $\beta_2$m binding increased in a DHA dose-dependent manner with each DHA treatment (Fig. 8). Figure 8 is an average of 8 experiments. Cells treated with 35 µM DHA were an average of 48% more fluorescent than untreated cells. The 40 µM and 45 µM DHA treatments were 57% and 65% more

fluorescent, respectively. Of importance is the dramatic linear increase in $\beta_2$m binding in response to DHA treatment (48-65% more fluorescent). The increase in $\beta_2$m binding is statistically significant and reproducible. In contrast, the treatment with the monounsaturated oleic acid had no significant effect on $\beta_2$m binding.

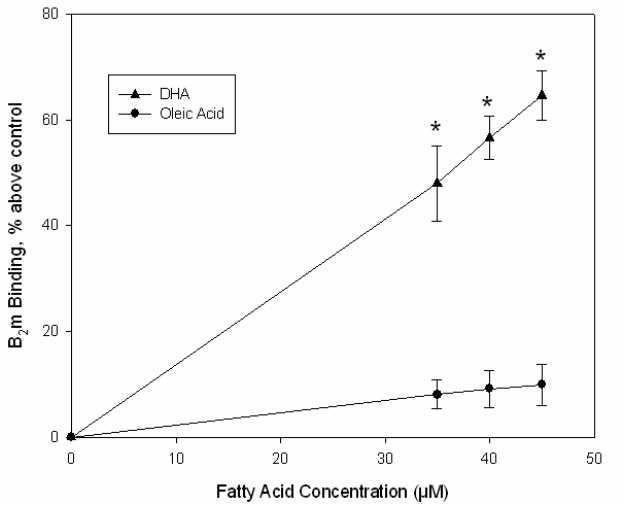


**Figure 8.** DHA increases $\beta_2$m binding to MHC I on the cell surface. EL4 cells were treated with 0-45 µM DHA and oleic acid for 48 hours at 37°C. $\beta_2$m binding was assayed as previously described. Overton percents were calculated by determining the percentage of cells in each treatment plot that were more fluorescent than the untreated cells. Data represent average of experiments (n=8). Error bars represent standard error. *One-way ANOVA was performed on data, n=8, and each DHA dose was determined to be statistically different from untreated cells, $P<0.05$.

**DHA increases AF6-88.5 binding to MHC I on the cell surface:**

The Mab clone AF6-88.5 binds to a conformational-epitope on the H-2K$^b$ $\alpha$ chain. EL4 cells were treated with fatty acid and AF6-88.5 binding was assayed by fluorescence flow cytometry. DHA-treated cells showed increased fluorescence compared to untreated and oleic acid treated cells (Fig. 9). Figure 9 shows the average of 7 experiments. Cells treated with 35 µM DHA were 34% more fluorescent than untreated cells. The 40 µM and 45 µM DHA treatments were 42% and 43% more

fluorescent, respectively. The fluorescence plots were gated on live cells, and to ensure that fluorescent antibody was not penetrating the cell, isotype control antibody binding was also assayed for each DHA treatment (Fig. 10). The isotype control antibody binding remained at background staining levels for each DHA treatment (Fig. 10). Of importance is the dramatic linear increase in AF6-88.5 binding in response to DHA treatment (34-43% more fluorescent). The increase in AF6-88.5 binding is statistically significant and reproducible. In contrast, the treatment with the monounsaturated oleic acid had no significant effect on AF6-88.5 binding.

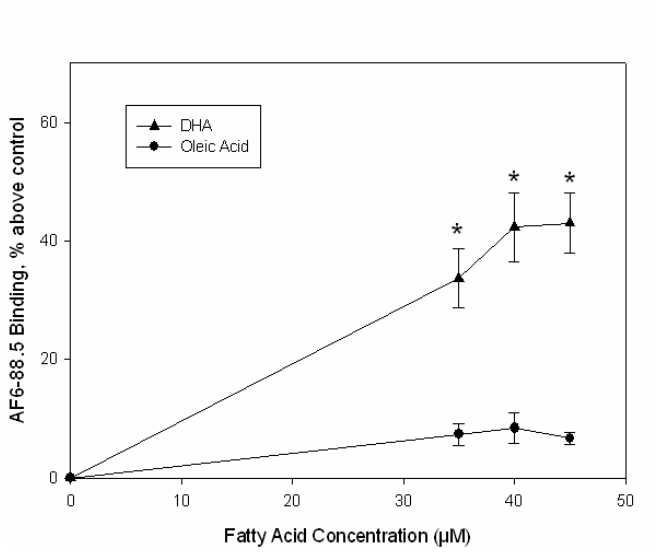


**Figure 9.** DHA increases AF6-88.5 binding to MHC I on the cell surface. EL4 cells were treated with 0-45 µM DHA or oleic acid and were then assayed for AF6-88.5 binding as previously described. Cells were then analyzed for fluorescence by flow cytometry. Overton percents were calculated by determining the percentage of cells in each treatment plot that were more fluorescent than the untreated cells. Data represent average of experiments (n=7). Error bars represent standard error. *One-way ANOVA was performed on the data, n=7, and each DHA dose was determined to be statistically different from untreated cells, $P<0.05$.

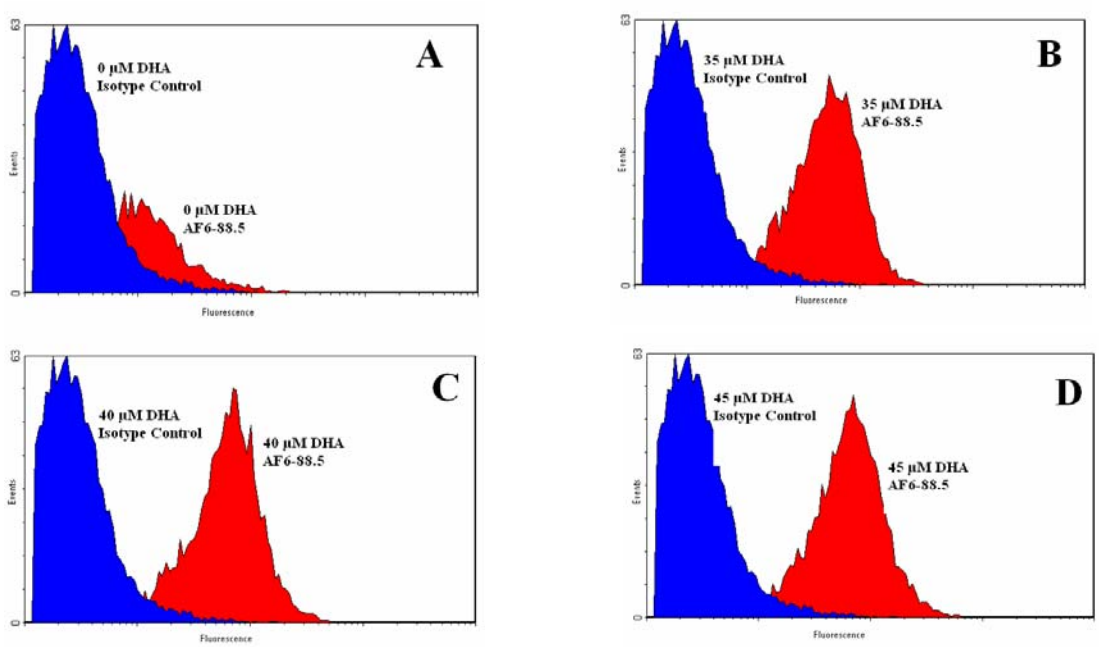


**Figure 10.** Example of overlay plots. AF6-88.5 binding is displayed by the peak on the right, and isotype control binding is displayed by the peak on the left. Overton percents were calculated by determining what percentage of each "positive plot" (AF6-88.5 binding) was more fluorescent than the control plot (Isotype control). **A)** 0 µM DHA treatment, 39% **B)** 35 µM DHA treatment, 85% **C)** 40 µM DHA treatment, 86% and **D)** 45 µM DHA treatment, 88%.

**DHA increases 28-14-8 binding to MHC I on the cell surface:**

The Mab clone 28-14-8 binds to a non-conformational epitope on the H-2D$^b$ α chain. EL4 cells were treated with fatty acid and assayed for 28-14-8 binding as previously detailed. DHA-treated cells showed increased fluorescence compared to untreated and oleic acid-treated cells (Fig. 11). Cells treated with 35 µM DHA were 33% more fluorescent than untreated cells. The 40 µM and 45 µM DHA treatments were 45% and 50% more fluorescent, respectively. The fluorescent plots were gated on live cells, and to ensure that fluorescent antibody was not penetrating the cell, isotype control antibody binding was also assayed for each DHA treatment (data not shown).

Of importance is the dramatic linear increase in 28-14-8 binding in response to DHA treatment (33-50% more fluorescent). The increase in 28-14-8 binding is statistically significant and reproducible. In contrast, the treatment with the monounsaturated oleic acid had no significant effect on 28-14-8 binding.

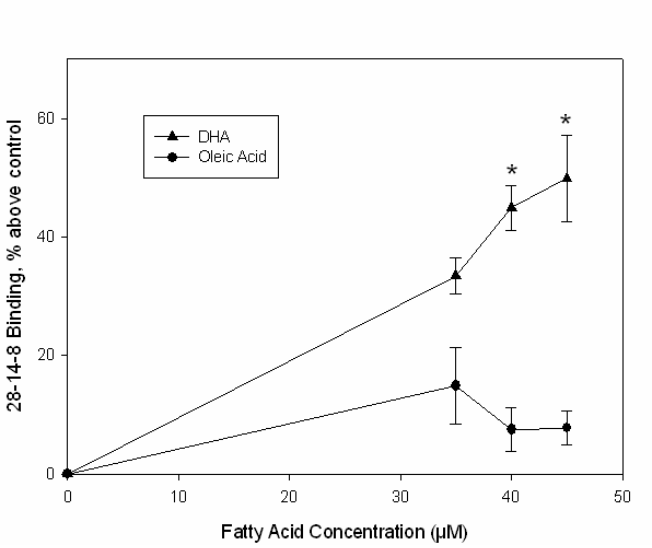


**Figure 11.** DHA increases 28-14-8 binding to MHC I on the cell surface. EL4 cells were treated with 0-45 µM DHA and oleic acid and were then assayed for 28-14-8 binding as previously described. Cells were analyzed for fluorescence by flow cytometry. Overton percents were calculated by determining the percentage of cells in each treatment plot that were more fluorescent than the untreated cells. Data represent average of experiments (n=5). Error bars represent standard error. *One-way ANOVA was performed on the data, n=5, and the 40 and 45 µM DHA doses were determined to be statistically different from untreated cells, $P<0.05$.

**DHA increases Mab binding of peptide-induced MHC I on the cell surface:**

The mutant mouse lymphoma cell line RMA-S shows a strongly reduced cell surface expression of H-2 class I molecules, although heavy and light chains of class I molecules are synthesized normally. This abnormality is due to the lack of the genes encoding TAP-2 proteins. Because RMA-S cells are TAP-2 deficient, they do not form functional TAP heterodimers and hence cannot efficiently supply cytosolic peptides for class I assembly in the ER. Exposure of this cell line to exogenous peptide results in the

increased expression of MHC I molecules on the cell surface, interpreted as peptide-induced assembly of class I molecules in the ER and subsequent transport to the cell surface.

A peptide dose response curve was determined by exposing RMA-S cells to 300-500 μM SIINFEKL peptide for 12 hours at 37°C. MHC I surface expression was then measured by AF6-88.5 binding. MHC I surface expression did increase in a peptide dose-dependent manner (Fig. 12). The 500 μM peptide dose was chosen for further experiments because it yielded 74% more fluorescence than those cells that were not exposed to peptide. Figure 13 shows the overlay plots of RMA-S cells exposed to peptide superimposed with those that were not exposed to peptide.

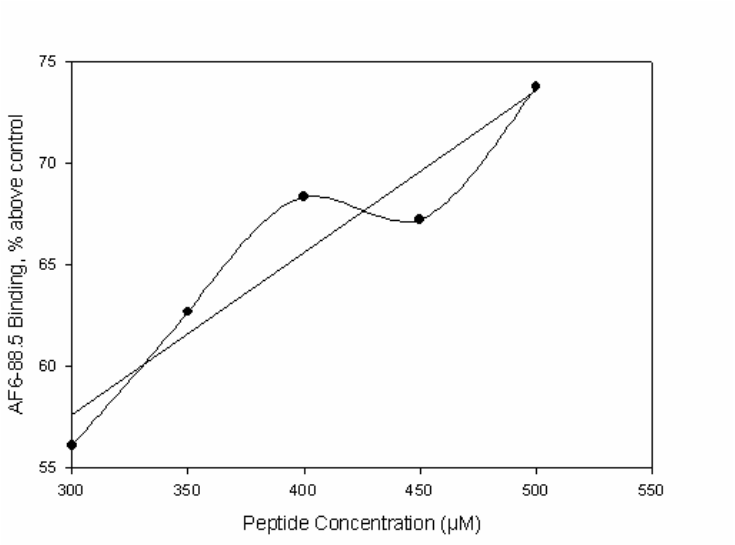


**Figure 12.** Peptide dose response curve. RMA-S cells were exposed to 300 to 500 μM SIINFEKL peptide for 12 hours at 37°C. After washing, the cells were incubated with FITC-conjugated AF6-88.5 and prepared as previously described. Overton percents were calculated by determining what percentage of peptide-exposed cells was more fluorescent than non-exposed cells. This graph is representative of one experiment.

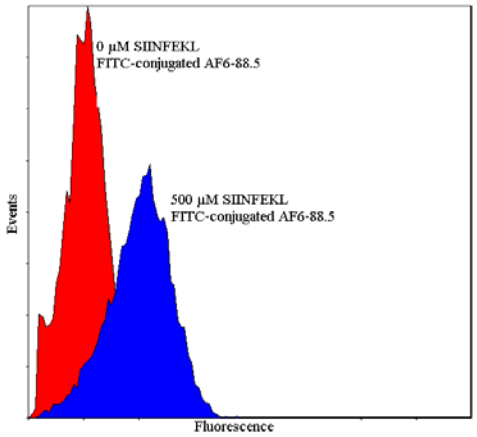


**Figure 13.** Overlay plots of peptide-exposed RMA-S cells vs. non-exposed cells. Peak on the left represents non-exposed cells treated with FITC-conjugated AF6-88.5 Mab. Peak on the right represents cells exposed to 500 µM SIINFEKL peptide for 12 hours at 37°C and then treated with FITC-conjugated AF6-88.5 Mab.

DHA and oleic acid treated cells were exposed to 500 µM SIINFEKL for 12 hours at 37°C. Negative control samples were not exposed to the peptide. The cells were then assayed for Mab binding as previously detailed.

DHA-treated cells showed higher fluorescence as compared to untreated and oleic acid-treated cells with both Mabs. Clone AF6-88.5 recognizes a conformational epitope (Fig. 14), and clone 28-14-8 recognizes an epitope that is not dependent on native α chain conformation (Fig. 15). Of importance is the dramatic linear increase in the binding of both Mabs in response to DHA treatment (9-21% more fluorescent for AF6-88.5 binding and 25-31% more fluorescent for 28-14-8 binding). The increase in Mab binding is statistically significant and reproducible. In contrast, the treatment with the monounsaturated oleic acid had no significant effect on Mab binding.

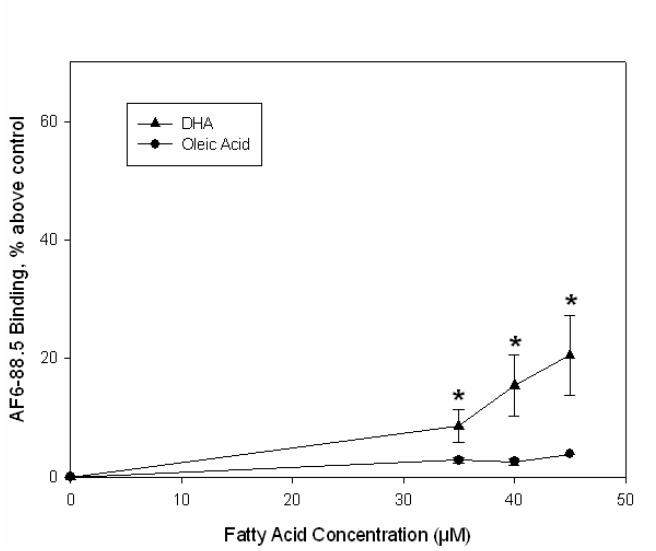


**Figure 14**. DHA increases AF6-88.5 binding to peptide-induced MHC I on the cell surface. RMA-S cells were treated with 0-45 µM DHA and oleic acid for 48 hours at 37°C. During the last 12 hours of this treatment, the cells were exposed to 500 µM SIINFEKL peptide. The cells were then assayed for AF6-88.5 binding as previously described, and analyzed for fluorescence by flow cytometry. Overton percents were calculated by determining the percentage of cells in each treatment plot that were more fluorescent than the untreated cells. Data represent an average of experiments (n=6). Error bars represent standard error. *One-way ANOVA was performed on the data, n=6, and it was determined that each DHA treatment was statistically different from the untreated cells, $P<0.05$.

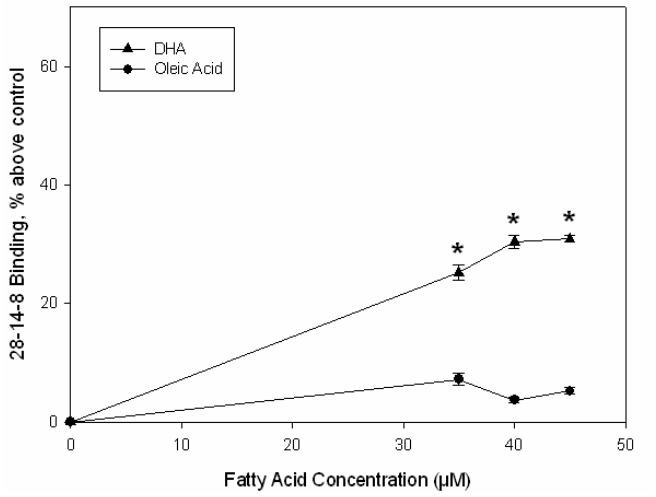


**Figure 15**. DHA increases 28-14-8 binding to peptide-induced MHC I on the cell surface. RMA-S cells were treated with DHA and peptide as previously described. They were then assayed for 28-14-8 binding and analyzed for fluorescence by flow cytometry. Overton percents were calculated by determining the percentage of cells in each treatment plot that were more fluorescent than the untreated cells. Data represent an average of experiments (n=3). Error bars represent standard error. *One-way ANOVA was performed on the data, n=3, and it was determined that each DHA treatment was statistically different from the untreated cells, $P<0.05$.

**α-Tocopherol eliminates DHA-associated increase of Mab binding to MHC I:**

α-Tocopherol, commonly referred to as vitamin E, is a strong antioxidant. To determine whether the effect of DHA on Mab binding assays and peptide-induced MHC I expression was an oxidative effect, and thus prevented by an antioxidant, 15 μg/ml of α-tocopherol was added to the cells prior to the 48 hour fatty acid treatment. The addition of α-tocopherol reversed the DHA-associated increase of Mab binding (Fig. 16 and 17) and peptide-induced MHC I expression (Fig. 18).

Figure 16 shows the addition of α-tocopherol to cells analyzed with the AF6-88.5 Mab binding assay. The effect of 35 μM DHA was decreased with the addition of α-tocopherol from 34% to 3% more fluorescence than untreated cells. The 40 μM DHA treatment was decreased from 42% to 4%, and the 45 μM DHA treatment was decreased from 43% to 3%. It is important to note the elimination of the DHA-associated increase in AF6-88.5 binding with the addition of α-tocopherol.

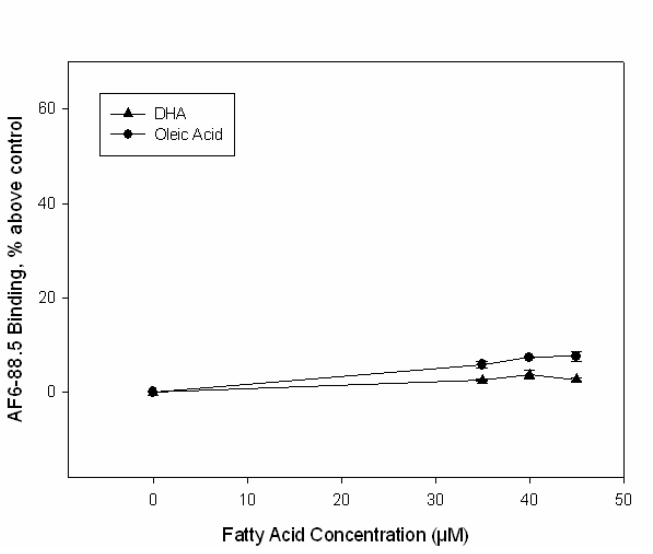


**Figure 16.** Addition of α-tocopherol eliminates DHA-associated increase in AF6-88.5 binding to MHC I on the cell surface. EL4 cells were treated with 0-45 μM DHA and oleic acid for 48 hours at 37°C in the presence of 15 μg/ml α-tocopherol. Cells were then assayed for AF6-88.5 binding as previously detailed. Overton percents were calculated by determining the percentage of cells in each treatment plot that were

more fluorescent than the untreated cells. Data represent average of experiments (n=2). Error bars represent the range of each data point.

Figure 17 shows the addition of α-tocopherol to the 28-14-8 Mab binding assay. Again, the addition of α-tocopherol eliminated the DHA-associated increase in 28-14-8 binding that was previously seen.

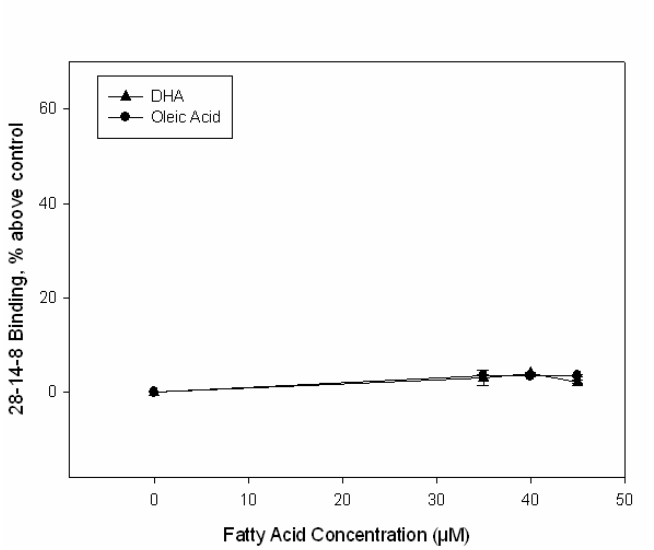


**Figure 17.** Addition of α-tocopherol eliminates DHA-associated increase in 28-14-8 binding to MHC I on the cell surface. EL4 cells were treated with 0-45 µM DHA and oleic acid for 48 hours at 37°C in the presence of 15 µg/ml α-tocopherol. The cells were then assayed for 28-14-8 binding as previously described. Overton percents were calculated by determining the percentage of cells in each treatment plot that were more fluorescent than the untreated cells. Data represent average of experiments (n=2). Error bars represent the range of each data point.

Figure 18 shows the addition of α-tocopherol to the peptide-induced MHC I expression assay. The addition of α-tocopherol to this assay eliminated the DHA-associated increase in Mab binding that was previously seen (Fig. 9, 11, 14, 15).

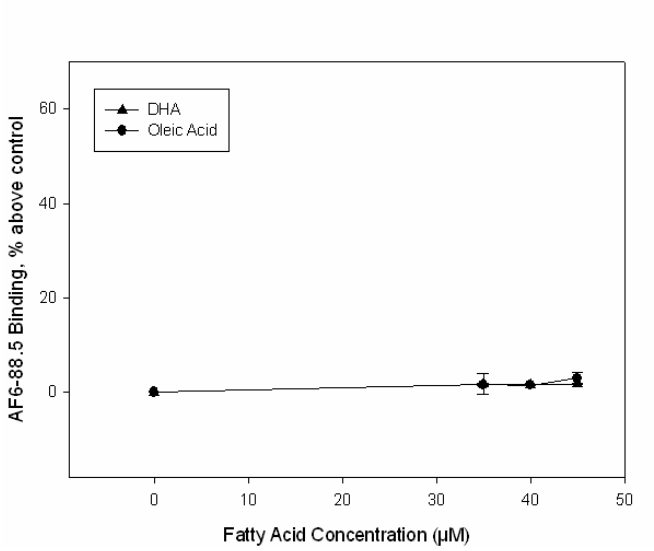


**Figure 18.** Addition of α-tocopherol eliminates DHA-associated increase in AF6-88.5 binding to peptide-induced MHC I on the cell surface. RMA-S cells were treated with 0-45 µM DHA and oleic acid for 48 hours at 37°C in the presence of 15 µg/ml α-tocopherol. During the last 12 hours of this treatment, the cells were exposed to 500 µM SIINFEKL peptide. The cells were then assayed for AF6-88.5 binding as previously described. Overton percents were calculated by determining the percentage of cells in each treatment plot that were more fluorescent than the untreated cells. Data represent an average of experiments (n=3). Error bars represent standard error.

The dose response for α-tocopherol was determined by adding 0 to 22.5 µg/ml α-tocopherol to EL4 cells being treated with 45 µM DHA. As shown in Figure 19, as the amount of α-tocopherol present increased, the DHA-associated effect on AF6-88.5 binding decreased. For this particular experiment, the reversal of DHA's effect seemed to level off at around 13% with 15 µg/ml α-tocopherol.

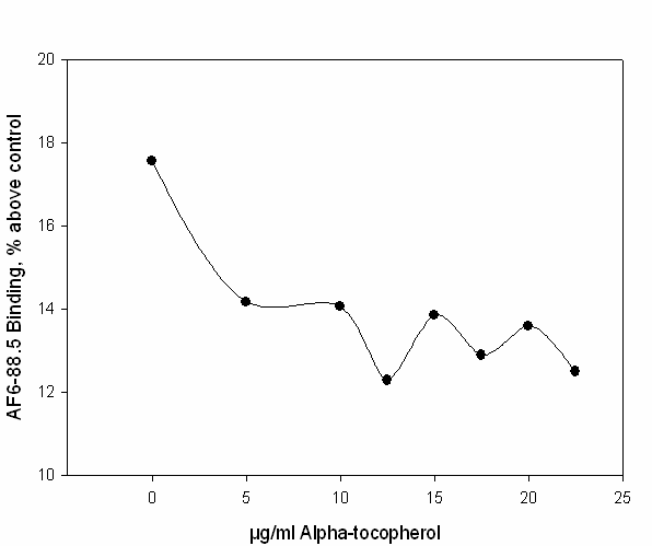


**Figure 19.** α-Tocopherol dose response curve. El4 cells were treated with 45 µM DHA in the presence of 0 to 22.5 µg/ml α-tocopherol. AF6-88.5 binding was measured as previously described. Overton percents were calculated by determining the percentage of cells in each treatment plot that were more fluorescent than the untreated cells.

α-Tocopherol also restored the scatter pattern of DHA-treated cells (Fig. 20). In the absence of α-tocopherol, 41% of DHA-treated cells were gated for fluorescence analysis (Fig. 6). However, with the addition of α-tocopherol, 75% of DHA-treated cells were gated (Fig. 20).

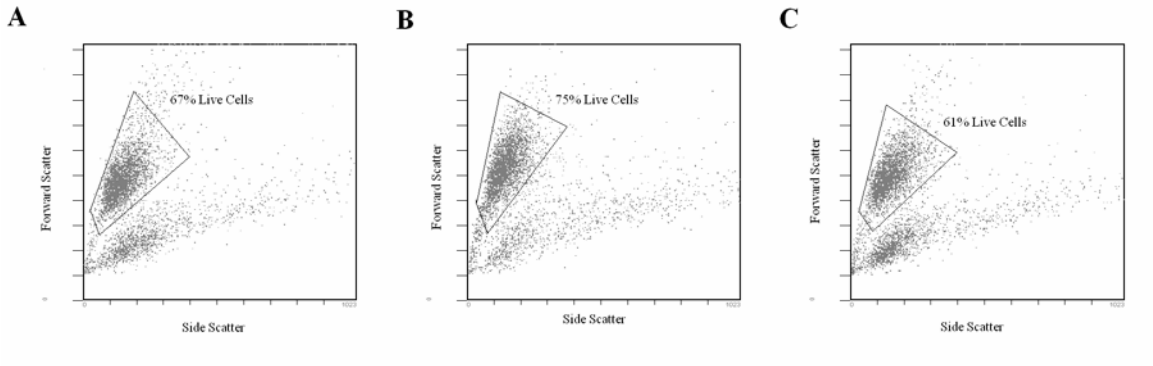


**Figure 20.** Scatter plots of α-tocopherol treated EL4 cells. A) Two-dimensional plot of forward versus side (90°) laser light scatter of 15 µg/µl α-tocopherol treated EL4 cells. The gate defines the cell population analyzed for fluorescence (67%). B) 45 µM DHA and 15 µg/µl α-tocopherol treated EL4 cells, 75% gated. C) 45 µM oleic acid and 15 µg/µl α-tocopherol treated EL4 cells, 61% gated. These graphs are representative of a single experiment.

**Summary of Results:**

In summary, it is evident that DHA increases $\beta_2$m and Mab binding. These increases occur in a DHA dose-dependent manner. The addition of $\alpha$-tocopherol eliminates this DHA-associated effect. The implications of these phenomena will be discussed later.

## DISCUSSION

The purpose of this study was to determine the effects of DHA on class I MHC structure and function by probing $\beta_2$m binding and Mab binding to MHC I on the EL4 cell surface and peptide-induced MHC I on the RMA-S cell surface. EL4 and RMA-S cells were cultured for 48 hours with 0-45 μM DHA or oleic acid. Murine to human β2m exchange and Mab binding were assessed by fluorescence flow cytometry. Peptide-induced MHC I expression was shown by fluorescent Mab binding after peptide-exposure to cells.

DHA-treated cells showed increased fluorescence compared to untreated and oleic acid-treated cells. Increased fluorescence indicates an increase in $\beta_2$m and Mab binding. As indicated by scatter plots, DHA-treated cells showed an increase in side scatter, representative of an increase in cell membrane complexity (Fig. 6). This cellular shift illustrates that DHA is having a dramatic effect on cell membrane properties.

This DHA-associated effect was further demonstrated by examining peptide-induced MHC I expression. The TAP-deficient cell line, RMA-S, was exposed to exogenous peptide to induce the surface expression of MHC I molecules. Fluorescent-labeled anti-MHC I Mab, clones AF6-88.5 and 28-14-8, detected the presence of these molecules. Again, DHA-treated cells showed increased fluorescence compared to untreated and oleic acid-treated cells (Fig. 14, 15).

Mab binding to MHC I was examined in two cells lines that assemble MHC I in very different ways. EL4 cells undergo "normal" MHC I assembly, while RMA-S cells undergo MHC I assembly in a TAP-deficient mechanism. A DHA-associated increase in

Mab binding was observed in both cases, which indicates that DHA's effect operates on MHC I no matter how it comes to the cell surface. At least one commonality between EL4 and RMA-S cells is the cell membrane.

It was originally believed that DHA's effect on the cell membrane was causing a conformational change in MHC I that resulted in increased $\beta_2$m and Mab clone AF6-88.5 binding (Fig. 8, 9). Mab clone AF6-88.5 recognizes a conformational epitope on the H-2K$^b$ $\alpha$ chain. However, Mab clone 28-14-8, which recognizes an epitope that is not dependent on native $\alpha$ chain conformation, also exhibits increased binding with DHA treated cells (Fig. 11). Thus, if the presence of DHA in membrane lipids induces a conformational change in MHC I, both epitopes are affected.

The addition of $\alpha$-tocopherol to the fatty acid treatment of the cells eliminated the DHA-associated increase in Mab binding in both EL4 cells and RMA-S cells exposed to exogenous peptide (Fig. 16, 17, 18). This result has many implications.

$\alpha$-Tocopherol is a strong antioxidant that intercalates into the cell membrane where it breaks the chain reaction of lipid peroxidation. It is well known that DHA is easily oxidized due to its six double bonds. The fact that the DHA-associated increase in Mab binding is eliminated by the addition of $\alpha$-tocopherol may suggest that DHA is having an oxidative effect on MHC I structure and function. However, since oxidation damages the cell membrane, it is unlikely that Mab binding to MHC I would increase under oxidative stress. The possibility that fluorescent Mab penetrates the damaged cell membrane is ruled out by the isotype control antibodies used in each experiment (Fig. 10).

A possible explanation for the DHA-associated increase in $\beta_2$m and Mab binding lies in the "PrOxI" hypothesis proposed by Teoh, et al (46). They hypothesize that the immunoproteasome, which is primarily responsible for generating peptides to be presented by MHC I molecules, targets oxidatively modified proteins for degradation (46). Thus, if the oxidation of DHA is affecting nearby proteins, these proteins would be targeted by the immunoproteasome for degradation into peptides that would then be presented by MHC I. An increase in presentable peptide might stimulate the assembly of class I MHC molecules to the cell surface resulting in an increase in $\beta_2$m and Mab binding (Fig. 21).

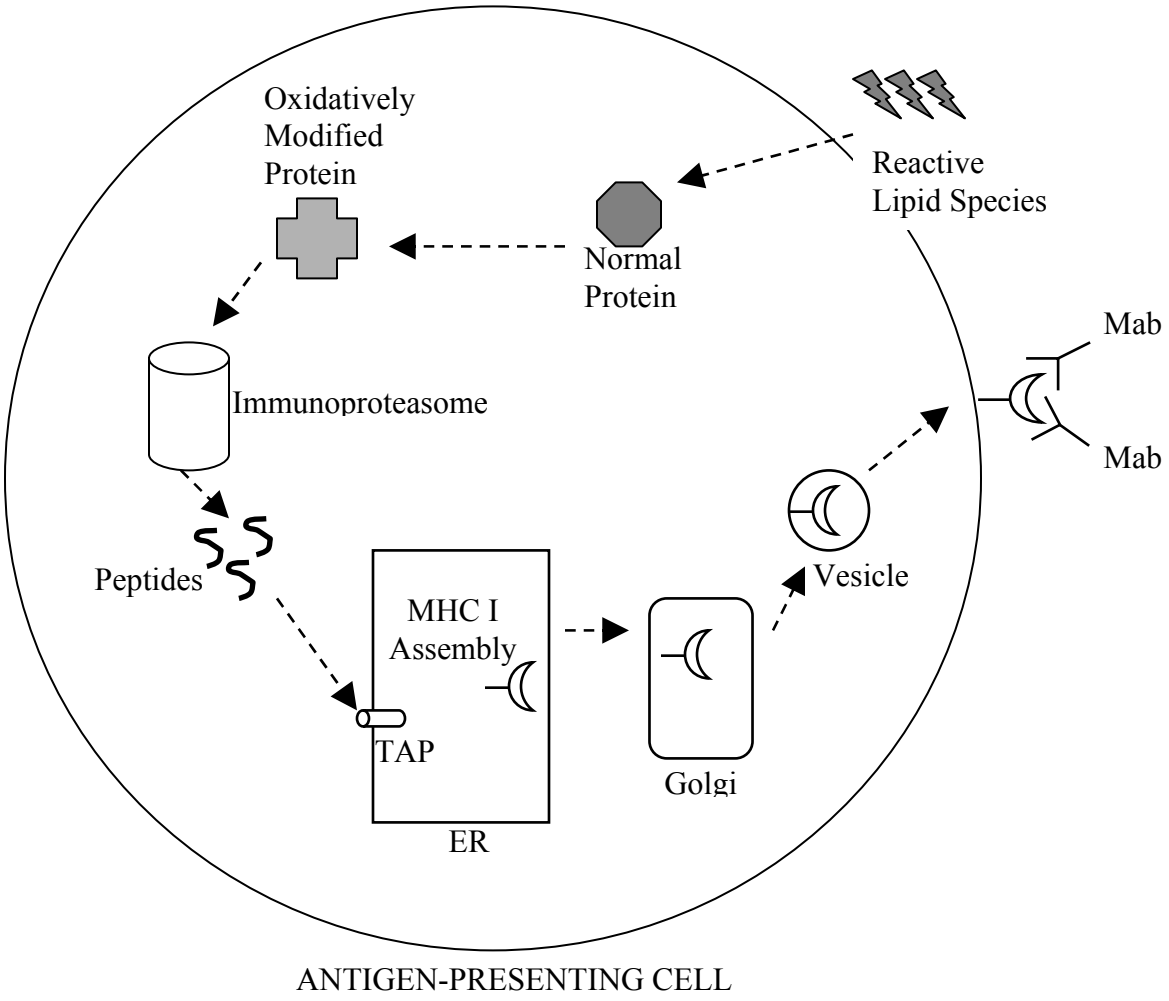


**Figure 21.** The protein oxidation and immunoproteasome or 'PrOxI' hypothesis of MHC-I antigen processing. DHA may cause normal proteins to be oxidatively modified and targeted for degradation by the immunoproteasome. The generated peptides are then transported into the ER by TAP and bind MHC I molecules. Fully assembled MHC I molecules are then transported to the Golgi and into vesicles that transport them to the cell membrane. Once on the cell surface, Mab readily binds the MHC I molecules (46).

This hypothesis may be responsible for the DHA-associated increase in $\beta_2$m and Mab binding to MHC I on EL4 cells. RMA-S cells, which are TAP-deficient, are unable to transport peptide into the ER through a normal mechanism. However, incubation with exogenous peptides in TAP-deficient cells can induce the release of nascent class I

molecules from the ER, suggesting that the peptide acts inside the ER to induce MHC I maturation from the ER to the cell surface (17). Thus, if an abundance of peptide is available from the degradation of oxidatively modified proteins, this peptide would induce the release of class I molecules from the ER. If such were the case in RMA-S cells, MHC I would be detectable on the surface of DHA-treated cells in the absence of exogenous peptide (SIINFEKL). The fact that no MHC I is detectable of the surface of DHA-treated RMA-S cells in the absence of exogenous peptide suggests that DHA is affecting RMA-S MHC I molecules in some other way.

DHA's effect on MHC I may be a structural effect rather than an oxidative effect. As seen in Figure 6, DHA has a dramatic effect on the cell membrane as represented by laser light side scatter. Specifically, it is known that DHA increases membrane fluidity and permeability and decreases membrane stability (33, 36-40). Since MHC I is a transmembrane protein, changes in these membrane properties may have an effect on MHC I conformation. Such a conformational change would alter the binding specificities of $\beta_2$m and Mabs. It has been previously suggested by Pascale, et al. that DHA played a role in altering MHC I conformation as shown by Mab binding (47).

In addition to its strong antioxidant properties, α-tocopherol also decreases membrane fluidity by intercalating into the cell membrane (48). The addition of α-tocopherol to DHA-treated cells would stabilize the membrane by decreasing membrane fluidity. This effect may explain the elimination of the DHA-associated increase of $\beta_2$m and Mab binding upon the addition of α-tocopherol to DHA-treated cells. Figure 20 shows the scatter patterns of cells treated with DHA in the presence of 15 μg/μl α-tocopherol. Compared to DHA-treated cells (with no α-tocopherol), these cells have

reduced membrane complexity. α-Tocopherol prevents the effect of DHA on the cell membrane and prevents the DHA-associated increase in Mab binding. This is strong evidence that the DHA-associated increase in $\beta_2$m and Mab binding is due to DHA's effect on membrane structure.

There are other possible causes for the increase of $\beta_2$m and Mab binding observed in DHA-treated cells that are worthy of mention. It is possible that DHA is directly causing an increase in MHC I biosynthesis rather than oxidants from DHA causing an increase in expression as previously discussed.

In conclusion, it is believed that this study has provided sufficient evidence that DHA causes an increase in $\beta_2$m and Mab binding to MHC I. It is predicted that this increase in binding indicates some change in MHC I (conformational or otherwise) that will affect the ultimate function of MHC I, which is to present antigen to $CD8^+$ T lymphocytes. These effects may alter the immune response in such a way as to prevent or improve the outcome of cancer and autoimmune disease. Further research needs to be conducted to gather more evidence towards the exact mechanism by which DHA effects MHC I structure and function.

**Suggestions for future research:**

This study has established that DHA does have an effect on $\beta_2$m and Mab binding to MHC I on the cell surface, but exact mechanism by which that effect occurs is not yet fully understood. Further experiments need to be performed to determine how DHA increases $\beta_2$m and Mab binding.

To determine if DHA is causing an increase in MHC I expression on the cell surface, the "on rate" of MHC I to the cell surface should be measured in DHA-treated cells versus untreated cells. Upon exposing DHA-treated RMA-S cells to exogenous peptide (to induce MHC I surface expression), samples could be stained for Mab binding and analyzed by flow cytometry at periodic time intervals. The rate at which MHC I appears in DHA-treated cells should be compared that in untreated cells.

Also, since the exact role of α-tocopherol in these assays has yet to be determined, antioxidants with different properties need to be tested. For instance, BHT (butylated hydroxytoluene) is an antioxidant that does not intercalate into the cell membrane but does break the chain reaction of lipid peroxidation, as does α-tocopherol (48). If BHT does not eliminate the DHA-associated increase in $\beta_2$m and Mab binding, it can be assumed that DHA is not having an oxidative effect on MHC I structure and function. On the other hand, another antioxidant, probucol, does enter the cell membrane but does not affect membrane stability or fluidity (48). If probucol does not eliminate the DHA-associated increase in $\beta_2$m and Mab binding, it can be assumed that DHA is affecting MHC I structure and function by changing membrane fluidity and stability.

To further explore the possibility that DHA is having an oxidative effect on MHC I structure and function, experiments using "pre-oxidized" DHA are being conducted. DHA will readily oxidize placed in an unsealed container under light for approximately one hour. This "pre-oxidized" DHA is then suspended in serum-free medium and added to cells, which are then incubated at 37°C for 48 hours. It is predicted that if DHA is having an oxidative effect on MHC I to cause an increase in $\beta_2$m and Mab binding, then pre-oxidized DHA will cause an even greater increase in $\beta_2$m and Mab binding.

Preliminary results suggest that the DHA-associated increase in $\beta_2$m and Mab binding is the same as or greater than that of pre-oxidized DHA. Again, this suggests that DHA-associated increase in $\beta_2$m and Mab binding is not due to an oxidative effect on MHC I structure and function.

Once the mechanism by which DHA affects MHC I structure and function is determined, further investigation into how DHA-enriched cells are able to stimulate a T cell response should be conducted. This could be performed in a mouse model system comparing the immune response of mice on DHA-rich diets to that of mice on normal diets.

## LITERATURE CITED


1. Goldsby RA, Kindt TJ, Osbourne BA, Kuby J (2003). Immunology 5th edition. New York: W.H. Freeman and Company.
2. Zinkernagel RM (1974). Immunological surveillance against altered self components by sensitized T lymphocytic choriomeningitis. Nature 51: 547-548.
3. Zinkernagel RM, Doherty PC (1979). MHC restricted cytotoxic T cells: studies on the biological role of polymorphic major transplantation antigens determining T cell restriction specificity, function, and responsiveness. Advan. Immunol. 27: 51-177.
4. Yu YY, Netuschil N, Lybarger L, Connally JM, Hansen TH (2002). Cutting Edge: Single chain trimers of MHC class I molecules form stable structures that potently stimulated antigen-specific T cells and B cells. J Immunol. 168(7): 3145-3149.
5. Garbozi DN, Biddison WE (1999). Shapes of MHC restriction. Immunity 10: 1-7.
6. Celia H, Wilson-Kubalek E, Milligan RA, Teyton L (1999). Structure and function of a membrane bound MHC class I molecule. Proc. Natl. Sci. USA 96: 5634-5639.
7. Schell TD, Mylin LM, Tevethia SS, Joyce S (2002). The assembly of functional $\beta_2$-microglobulin-free MHC class I molecules that interact with peptides and $CD8^+$ T lymphocytes. International Immunology 14(7): 755-782.
8. Shields MJ, Moffat LE, Ribaudo RK (1998). Functional comparison of bovine, murine, and human $\beta_2$-microglobulin: interactions with murine MHC I molecules. Molecular Immunology 35: 919-928.
9. Cook JR, Myers NB, Hansen TH (1998). Peptide ligand structure influences the exchange of $\beta_2$-microglobulin by cell surface $K^b$. Molecular Immunology 35:929-934.
10. Rammensee HG, Falk K, Rötzschke O (1993). Peptides naturally presented by MHC class I molecules. Annu. Rev. Immunol. 11:213-244.
11. Van Bleek GM, Nathenson SG (1990). Isolation of an immunodominant viral peptide from the class I H-$2K^b$ molecule. Nature 348: 213-216.
12. Rötzschke O, Falk K, Stevanovic S, Jung G, Walden P, Rammensee HG (1991). Exact prediction of a natural T cell epitope. Eur. J. Immunol. 21: 2891-2894.
13. Wallny HJ (1992). Investigation of the MHC Class I molecule and the processing of histocompatible antigen. Thesis. Univ. Tübingen, Germany.
14. Townsend A, Ohlen C, Bastin J, Ljunggren HG, Foster L, Karre K (1989). Association of class I major histocompatibility complex heavy and light chains induced by viral peptides. Nature 340: 443-448.
15. Chicz R, Urban R (1994). Analysis of MHC-presented peptides:

applications in autoimmunity and vaccine development. Immunol. Today 15: 155-160.
16. Pfrefer JD, Wick MJ, Roberts RL, Findlay K, Normark SJ, Harding CV (1993). Phagocytic processing of bacterial antigens for class I MHC presentation to T cells. Nature 361: 359-362.
17. Levitt JM, Howell DD, Rodgers JR, Rich RR (2001). Exogenous peptides enter the endoplasmic reticulum of TAP-deficient cells and induce the maturation of nascent MHC class I molecules. Eur. J. Immunol. 31: 1181-1190.
18. Luft T, Rizkalla M, Tai TY, Chen Q, MacFarlan RI, Davis ID, Maraskovsky E, Cebon E (2001). Exogenous peptides presented by transporter associated with antigen processing (TAP)-deficient and TAP-competent cells:intracellular loading and kinetics of presentation. J Immunol. 167: 2529-2537.
19. Day PM, Yewdell JW, Porgador RN, Germain RN, Bennink JR (1997). Direct delivery of exogenous MHC class I molecule binding oligopeptides to the endoplasmic reticulum of viable cells. Proc. Natl. Sci. USA 94: 8064.
20. Bang HO, Dyerberg J, Sinclair HM (1980). The composition of the Eskimo food in north western Greenland. American Journal of Clinical Nutrition 33: 2657-2661.
21. Dyerberg J, Bang HO (1979). Haemostatic function and platelet polyunsaturated fatty acids in Eskimos. Lancet 2: 433-435.
22. McLennan P, Howe P, Abey W, Ardena M, Muggli R, Raederstorff D, Mano M, Rayner T, Head R (1996). The cardiovascular protective role of docosahexaenoic acid. Eur. J. Pharmacol. 300: 83-89.
23. Zerouga M, Stillwell W, Stone J, Powner A, Dumaual AC, Jenski LJ (1996). Phospholipid class as a determinant in docosahexaenoic acid's effect of tumor cell viability. Anticancer Res. 16: 2863-2568.
24. Kremer JM, Lawrence DA, Jubiz W, DiGiacomo R, Rynes R, Bartholomew LE, Sherman M (1990). Dietary fish oil and olive oil supplementation in patients with rheumatoid arthritis: Clinical and immunological effects. Arthritis Rheum. 33: 810-820.
25. Yokoyama A, Hamazaki T, Oshita A, Kohno N, Sakai K, Zhao GD, Katayama H, Hiwad K (2000). Effect of aerosolized docosahexaenoic acid in a mouse model of atopic asthma. Int. Arch. Allergy Immunol. 123: 327-332.
26. Das UN (1994). Beneficial effect of eicosapentaenoic and docosahexaenoic acids in management of systemic lupus erythematosus and its relationship to the cytokine network. Prostaglandins Leukot. Essent. Fatty Acids 51: 207-213.
27. Pawlosky RJ, Salem Jr. N (1995). Ethanol exposure causes a decrease in docosahexaenoic acid and an increase in docosapentaenoic acid in feline brains and retinas. Am J Clin Nutr 61: 1284-1289.
28. Caulder PC (1996). Effects of fatty acids and dietary lipids on the

cells of the immune system. Proceedings of Nutrition Society 55: 127-150.
29. Breckenridge WC, Gombos G, Morgan IG (1972). The lipid composition of the adult rat brain synaptosomal membranes. Biochim Biophys Acta 266: 695-707.
30. Neill AR, Masters CJ (1973). Metabolism of fatty acids by ovine spermatozoa. J Reprod. Fertil. 34: 279-287.
31. Wiegand RD, Anderson RE (1983). Phospholipid molecular species of frog rod outer segment membranes. Exp. Eye Res. 37: 159-173.
32. Salem Jr. N, Kin HY, Yergey JA (1986). DHA: membrane function and metabolism. In: Simopolus AP, Kifer RR, Martin RE (Eds.). Health effects of polyunsaturated fatty acids in seafoods. Academic Press, New York pp. 319-351.
33. Stillwell W, Wassall SR (2003). DHA: Membrane properties of a unique fatty acid. Chemistry and physics of lipids 126: 1-27.
34. Stillwell W, Jenski LJ, Crump FT, Ehringer W (1997). Effect of DHA on mouse mitochondrial membrane properties. Lipids 32: 497-506.
35. Tahin QS, Blum M, Carafoli E (1981). The fatty acid composition of subcelluar membranes of rat liver, heart, and brain: diet-induced modification. Eur J Biochem 121: 5-13.
36. Brown MF (1994). Modulation of rhodopsin function by properties of the membrane bilayer. Chem Phys Lipids 73: 159-180.
37. Calder OC, Yaqoob P, Harvey DJ, Watts A, Newsholme EA (1994). Incorporation of fatty acuds by concanavalin A-stimulated lymphocytes and the effect on fatty acid composition and membrane fluidity. Biochem J 300: 509-518.
38. Sobajima T, Tamiya-Koizumi K, Ishihara H, Kojima K (1986). Effects of fatty acid modification of ascites tumor cells on pulmonary metastasis in rat. Jpn J Cancer Res 77: 657-663.
39. Yorek M, Leeney E, Dunlap J, Ginsberg B (1989). Effect of fatty acid composition on insulin and IGF-1 binding in retinoblastoma cells. Invest. Pphthalmol. Vis. Sci. 30: 2087-2092.
40. Stillwell W, Ehringer WD, Jenksi LJ (1993). DHA increase permeability of lipid vesicles and tumor cells. Lipids 28: 103-108.
41. Holte LL, Peter SA, Sinnwell TM, Gawrisch K (1995). 2H nuclear magnetic resonance order profiles suggest a change of molecular shape for phosphatidylcholines containing a polyunsaturated acyl chain. Biophys J 68: 2396-2403.
42. Mitchell DC, Gawrisch K, Litman BJ, Salem Jr. N (1998). Why is DHA essential for nervous system function? The molecular structure of phospholipids and the regulation of cell function. Biochem Soc. Trans. 26: 365-370.
43. Mitchell DC, Litman BJ (2001). Modulation of receptor signaling by phospholipid acyl chain composition. In: Mostofsky D, Yehuda S, Salem Jr. N (Eds.) Fatty acids: physiological and behavioral functions. Humana Press Inc., Totowa, NJ pp 23-40.

44. Jenski, LJ, Studevant LK, Ehringer WD, Stillwell W (1993). Omega-3 fatty acid modification of membrane structure and function: dietary manipulation of tumor cell susceptibility to cell and complement-mediated lysis. Nutr Cancer 19: 135-146.
45. Jenski LJ, Zerouga M, Stillwell W (1995). Omega-3 fatty acid containing liposomes in cancer therapy. Proc. Soc. Exp. Biol. Med. 210: 227-233.
46. Teoh CY, Davies KJ (2004). Potential roles of protein oxidation and the immunoproteasome in MHC class I antigen presentation: the 'PrOxI' hypothesis. Archives of Biochemistry and Biophysics. 423: 88-96.
47. Pascale AW, Ehringer WD, Stillwell W, Sturdevant LK, Jenski LJ (1993). Omega-3 fatty acid modification of membrane structure and function. II. Alteration by Docosahexaenoic acid of tumor cell sensitivity to immune cytolysis. Nutr. Cancer 19: 147-157.
48. van Aalst JA, Burmeister W, Fox PL, Graham LM (2004). α-Tocopherol preserves endothelial cell migration in the presence of cell-oxidized low -density lipoprotein by inhibiting changes in cell membrane fluidity. Journal of Vascular Surgery 39: 229-237.